



Ethaselen: a novel organoselenium anticancer agent targeting thioredoxin reductase 1 reverses cisplatin resistance in drug-resistant K562 cells by inducing apoptosis*

Suo-fu YE^{†1,2}, Yong YANG³, Lin WU³, Wei-wei MA^{1,2}, Hui-hui ZENG^{†‡1,2}

(¹State Key Laboratory of Natural and Biomimetic Drugs, Peking University, Beijing 100191, China)

(²School of Pharmaceutical Sciences, Peking University, Beijing 100191, China)

(³Keaise Clinical Examination Lab, Wuhan 430000, China)

[†]E-mail: pkuyesuofu@163.com; zenghh@bjmu.edu.cn

Received Feb. 19, 2016; Revision accepted May 4, 2016; Crosschecked Apr. 24, 2017

Abstract: It has been reported that Ethaselen shows inhibitory effects on thioredoxin reductase (TrxR) activity and human tumor cell growth. In order to find an efficient way to reverse cisplatin resistance, we investigated the reversal effects of Ethaselen on cisplatin resistance in K562/cisplatin (CDDP) cells that were established by pulse-inducing human erythrocyte leukemic cell line K562, which are fivefold more resistant to cisplatin compared to K562 cells. The morphology and growth showed that the adhesion of K562/CDDP further decreased while the cell volume increased. The proliferation of K562/CDDP is strengthened. The antitumor activities *in vitro* were assessed by MTT (3-(4,5-dimethylthiazol-2-yl)-2,5-diphenyltetrazolium bromide) assay and combination index (CI), showing the significant synergic effects of cisplatin and Ethaselen. Focusing on apoptosis, a series of comparisons was made between K562 and K562/CDDP. Cisplatin induced higher reactive oxygen species (ROS) generation in K562 and subsequently induced the formation of mitochondrial permeability transition pores (PTPs). In addition, cisplatin increased the ratio of Bax to Bcl-2 in K562, which can influence the mitochondrial membrane permeability. PTP formation and mitochondrial membrane permeabilization eventually resulted in the release of cytochrome *c* and activation of the Caspase pathway. However, these effects were not clearly seen in K562/CDDP, which may be the reason for the acquired CDDP resistance. However, Ethaselen can induce a high level of ROS in K562/CDDP by TrxR activity inhibition and increased ratio of Bax to Bcl-2 in K562/CDDP by nuclear factor κ B (NF- κ B) suppression, which subsequently induces the release of cytochrome *c* in K562/CDDP. This response is partly responsible for the reversal of the cisplatin resistance in K562/CDDP cells.

Key words: Cisplatin resistance; Cisplatin; Bcl-2; Cytochrome *c*; Ethaselen

<http://dx.doi.org/10.1631/jzus.B1600073>

CLC number: R9


1 Introduction

Cisplatin, a potent antitumor alkylating agent, is widely used for the clinical treatment of many malignancies, such as testicular, ovarian, head and

neck, bladder, esophageal, and small cell lung cancers. Cisplatin exerts its anticancer activity by forming 1,2-intrastrand cisplatin–DNA cross-links (Mantri *et al.*, 2007; Yaneva *et al.*, 2007; Harrington *et al.*, 2010). However, a serious limitation in cancer chemotherapy with cisplatin is the development of drug resistance. Furthermore, the dose escalation required to overcome even a small increase in resistance of a tumor to cisplatin can cause severe toxicities in patients (Yeh and Cheng, 1997; Miyata *et al.*, 2012). Therefore, understanding the molecular basis of cisplatin resistance

[‡] Corresponding author

* Project supported in part by the National Natural Science Foundation of China (No. 81372266) and the National Science and Technology Major Project of the Ministry of Science and Technology of China (No. 2011zx09101-001-03)

 ORCID: Suo-fu YE, <http://orcid.org/0000-0001-7661-6272>

© Zhejiang University and Springer-Verlag Berlin Heidelberg 2017

and finding an efficient method to overcome this resistance can improve the clinical effectiveness of this anticancer drug. Unfortunately, the mechanism of cisplatin resistance is a complex biological process involving multiple factors (Chao *et al.*, 1991; Torigoe *et al.*, 2005; Haslehurst *et al.*, 2012; Oiso *et al.*, 2014) and still remains largely unclear.

The induction of apoptosis in cancer cells is thought to be fundamental to the success of the treatment of the disease. The Bcl-2 family members are intimately involved in the apoptosis, but the role of these proteins in drug-induced death is controversial, including anti-apoptotic proteins such as Bcl-2, Bcl-XL, and Bcl-W, and pro-apoptotic proteins such as Bax, Bad, Bid, and Bim (Chu, 1994; Bargou *et al.*, 1995; Tilly *et al.*, 1995; Tao *et al.*, 1997; Hahn *et al.*, 2003; Dumay *et al.*, 2006; Heath-Engel *et al.*, 2008; Tanaka *et al.*, 2010; Chen *et al.*, 2014; Zheng *et al.*, 2015). It is certain that the Bcl-2 family of proteins is closely related to the regulation of cell death by inducing apoptosis, which is initiated by the release of cytochrome *c* from mitochondria. However, the relationship between the altered expression of apoptosis-regulating proteins and subsequent resistance to apoptosis still needs to be tested and studied.

As a novel potent antitumor candidate targeting thioredoxin reductase (TrxR), Ethaselen (1,2-[bis(1,2-benzisoselesazolone-3(2H)-ketone)]ethane; BBSKE) has shown good antitumor effects in many cancer models (Wang *et al.*, 2012). It was first prepared by our group and now has entered clinical trial Phase II. Ethaselen was designed to inhibit mammalian TrxR activity by selectively targeting SeCys498/Cys497, the C-terminal active sites of mammalian TrxR, with high binding potential (Shi *et al.*, 2003; Zhao *et al.*, 2006; Xing *et al.*, 2008). Ethaselen was found to inhibit TrxR activity in several human carcinoma cell lines and tumor-bearing mouse models (Shi *et al.*, 2003; Zhao *et al.*, 2006). Furthermore, TrxR inactivation by Ethaselen correlates with cell death/apoptosis, including A549 (human lung cancer), HeLa (human cervical cancer), BGC823 (human stomach adenocarcinoma), HL60 and K562 (human leukemia), LoVo (human colon cancer), Bel-7402 (human epithelial hepatoma), and Tca8113 (human tongue cancer) cells (Shi *et al.*, 2003; Zhao *et al.*, 2006; Xing *et al.*, 2008; Fu *et al.*, 2011; Wang *et al.*, 2011; 2012). Moreover, a synergistic effect has been observed in the study of

the combination of Ethaselen and cisplatin (CDDP) *in vivo*. Studies have shown that the antitumor efficacy of cisplatin on the stomach cancer cell line BGC-823, the human lung cancer cell line PG-BE1, the subcutaneous transplanted lung cancer cell line A459 in the nude mice, and the human colon adenocarcinoma cell line LoVo would be further enhanced through synergetic combination with Ethaselen (Tan *et al.*, 2010). These previous studies have indicated that there is a close link of the antitumor mechanism between Ethaselen and CDDP, suggesting that Ethaselen may be a potential and efficient method for reversing cisplatin resistance.

In the present study, we established cisplatin-resistant K562 cells and attempted to clarify the relationship between apoptosis and drug resistance in K562 cells. The expression patterns of the apoptosis-regulating proteins were analyzed to elucidate the mechanism of cisplatin-induced resistance. Furthermore, a possible effective way of reversing cisplatin resistance by Ethaselen was studied in order to provide a potential clinical application of Ethaselen-cisplatin combined chemotherapy.

2 Materials and methods

2.1 Chemicals and antibodies

Ethaselen (Fig. 1) was previously synthesized in our lab and verified by high-performance liquid chromatography (HPLC) (Shi *et al.*, 2003). Ethaselen was dissolved in 20 mmol/L in dimethyl sulfoxide (DMSO). Cyclosporin A (CsA) and 2',7'-dichlorodihydrofluorescein diacetate (DCFH-DA) were purchased from Sigma-Aldrich (Shanghai, China), and were dissolved in 5 and 20 mmol/L in HPLC-grade DMSO, respectively. The mammalian protease inhibitor cocktail was bought from Amresco Inc. (Solon, USA). Antibodies against Caspase-3 were purchased from Cell Signaling Technology (Shanghai, China). Antibodies against Bax, Bcl-2, and cytochrome *c* were bought from Santa Cruz Biotechnology Inc. (Shanghai, China), and β -actin was purchased from OriGene Technologies (Beijing, China).

2.2 Cell culture

Human erythrocyte leukemic cell line K562 and K562/CDDP were grown in RPMI-1640 medium

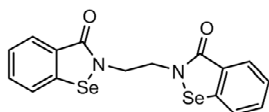


Fig. 1 Chemical structure of Ethaselen (BBSKE)

supplemented with 10% fetal bovine serum (FBS) in 5% CO₂ atmosphere at 37 °C. K562/CDDP cells were established in our laboratory by pulsed induction (Du *et al.*, 2007) and exposed to the final concentration of 30 μmol/ml cisplatin for six months.

2.3 Cell growth curves and population doubling time

K562, K562/CDDP (without CDDP), and K562/CDDP (exposed to 30 μmol/ml cisplatin) were obtained in the logarithmic phase with a cell density of 2000 cells/ml and seeded into 96-well plates (200 μl/well). MTT (3-(4,5-dimethylthiazol-2-yl)-2,5-diphenyltetrazolium bromide; Amresco Inc., Solon) assay was conducted each day for the next eight days. The cell growth curves were drawn with time as *X*-axis and the average absorbance of 16 replicates as *Y*-axis: the population doubling time (DT)=(*t*-*t*₀)×log2/(log*N*-log*N*₀), where *t* and *t*₀, respectively, represent the time of culture termination and beginning, and *N* and *N*₀ represent the numbers of cells at *t* and *t*₀, respectively.

2.4 Cell morphology

K562 and K562/CDDP, taken from logarithmic phase cells, were used to observe the cell morphology under a 10×40-fold inverted fluorescence microscope.

2.5 Cell growth inhibition assays

Cells in the exponential growth phase were plated into 96-well plates at 5000 cells/well. After exposure to various concentrations of CDDP or Ethaselen separately and in combination (the molar ratio of CDDP to Ethaselen was 10: 1) for 24, 48, and 72 h, the growth inhibition activities of different drug treatments on K562 and K562/CDDP cells were determined using MTT assay. The data were recorded on a microplate reader DNM-9602 (Beijing Perlong New Technology Co., Ltd., Beijing, China) at 570 nm. The inhibitory rate was calculated using the software Origin 7.5 (OriginLab, USA).

2.6 Median effect analysis

The combination index (CI) was used to explore the drug interaction in combinations including synergy (CI<0.95), additivity (0.95≤CI≤1.05), or antagonism (CI>1.05).

The CI value was calculated as $CI = D_1/D_{x1} + D_2/D_{x2}$, where *D*₁ and *D*₂ are the dosages of drugs used in combination to get a certain antitumor effect, respectively, and *D*_{*x*1} and *D*_{*x*2} are the dosages of drugs used separately to get same antitumor effect, respectively.

2.7 Flow cytometric analysis of apoptosis and intracellular ROS levels

Cells undergoing apoptosis under various treatment conditions were prepared by the Annexin V-propidium iodide (PI) apoptosis detection kit according to the manufacturer's instructions.

After exposure to CDDP alone or to the combination of CDDP and Ethaselen, cells were harvested, washed once with ice-cold phosphate buffer saline (PBS), and incubated with DCFH-DA (100 μmol/L final concentration) at 37 °C for 15 min in the dark (Sainz *et al.*, 2003). Then the cells were washed again and maintained in 1 ml PBS. The reactive oxygen species (ROS) levels were determined using the Guava EasyCyte Plus flow cytometry system (Merck Millipore).

2.8 Western blot analysis

After drug treatment, the whole cell lysates of K562 and K562/CDDP cells were prepared by lysing cells in the radioimmunoprecipitation assay (RIPA) buffer (137 mmol/L NaCl, 1 mmol/L ethylene diamine tetraacetic acid (EDTA), 10 mmol/L Tris-HCl (pH 7.4), 0.1% sodium dodecyl sulfate (SDS), 1% (0.01 g/ml) sodium deoxycholate, 1% Triton X-100). Mammalian protease inhibitor cocktail was added to the buffer according to the manufacturer's instructions.

In order to get the cytosolic and mitochondrial fractions, K562 and K562/CDDP cells were suspended in 400 μl of the isotonic buffer (250 mmol/L sucrose, 10 mmol/L Tris-HCl, 1 mmol/L EDTA) including protease inhibitors, and lysed by a tight-fitting Dounce homogenizer. The supernatant was obtained by centrifuging the lysate at 1000g for 10 min, and subsequently centrifuged at 17000g for 15 min to separate the cytosolic fraction and mitochondrial sediment which was further lysed by 150 μl RIPA.

Protein concentration was determined by the BCA (bicinchoninic acid) method. The cellular protein sample (50 μg) was subjected to sodium dodecyl sulfate-polyacrylamide gel electrophoresis (SDS-PAGE), and the separated proteins were subsequently electrically transferred to a polyvinylidene (PVDF) membrane. The membrane was blocked by nonfat milk and incubated with suitable primary and secondary antibodies. The electrochemiluminescence (ECL) signals were recorded on X-ray films.

2.9 Statistical analysis

Data of independent experiments were expressed as mean \pm standard deviation (SD) and analyzed using a two-tailed *t*-test. *P*-values less than 0.05 were considered statistically significant.

3 Results and discussion

3.1 Resistant cells and parental cell growth curves and population doubling time

The growth curves of the parental cell line K562 and resistant cells K562/CDDP without drugs (Fig. 2) indicated that the proliferative capacities of resistant cells K562/CDDP were higher than those of the parental cells K562. When cultured with the drug in the medium to maintain drug resistance, the proliferative capacities of the resistant cells K562/CDDP were lower than those of the parental cells K562 (Fig. 2 and Table 1), but there was no significant difference ($P>0.05$).

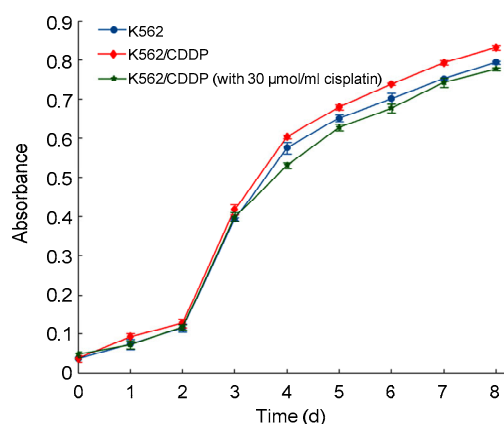


Fig. 2 Growth curves of K562, K562/CDDP, and K562/CDDP with 30 $\mu\text{mol/ml}$ cisplatin

Data are expressed as mean \pm SD ($n=3$)

Table 1 Cell population doubling time

Cells	Doubling time (h)
K562	30.459 \pm 7.722
K562/CDDP	29.399 \pm 8.487 ^a
K562/CDDP (with cisplatin)	36.252 \pm 7.993 ^a

^a $P>0.05$, vs. K562, suggesting no significant difference

3.2 Cell morphology

Under a 10 \times 40-fold inverted microscope (Fig. 3), K562 and K562/CDDP cells were the translucent circular suspension cells. The adhesion of K562 cells was weak, and the cells were dispersed in the medium and less attached to the cell culture flask. The cell volume was small. Compared with K562, the adhesion of K562/CDDP was further decreased while the cell volume increased.

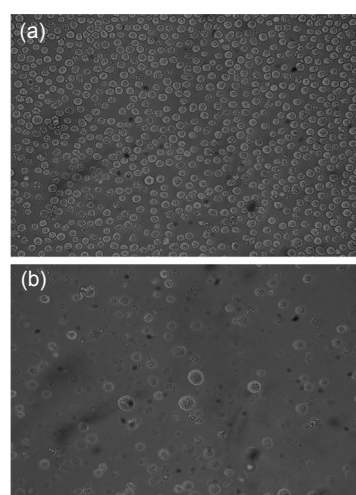


Fig. 3 Morphologies of K562 (a) and K562/CDDP (b) under a 10 \times 40-fold inverted microscope

3.3 Drug sensitivity testing by MTT method in vitro and median effect analysis

From Fig. 4, it can be seen that with the increase of drug action time, the effects of CDDP, Ethaselen, and their combinations on the K562 and K562/CDDP cells gradually increased, especially obviously in Figs. 4d–4f. The shapes of dose-response curves of the parental and resistant K562 cells to the same drug or drug combination had some differences, which showed the resistance characteristics of the drug-resistant cells.

As can be seen from Table 2, K562/CDDP produced a certain degree of resistance to CDDP, Ethaselen, and their combination. The half-maximum inhibitory concentration (IC₅₀) of CDDP on K562/CDDP was 5.34 times that of CDDP on K562 ($P<0.01$) and the IC₅₀ of Ethaselen on K562/CDDP was 1.36 times that of Ethaselen on K562 ($P<0.01$). The dosages of the combination of CDDP and Ethaselen added to K562 and K562/CDDP cells to produce a specific inhibitory effect were lower than when they were used separately. The CI of the drug combination group was 0.169 on K562 cells and 0.107 on K562/CDDP cells, showing significant synergism ($P<0.05$) of CDDP and Ethaselen on the two types of cells. By the presence of small amounts of Ethaselen, the IC₅₀ of CDDP on K562/CDDP cells could reduce from 260.986 to 12.368, which indicated

that Ethaselen can reverse cisplatin resistance in drug-resistant K562 cells.

3.4 Flow cytometric analysis of apoptosis

After treating with the vehicle (control), 50 μmol/L CDDP, and the combination of 1.5 μmol/L Ethaselen and 15 μmol/L CDDP for 48 h, K562/CDDP cells were harvested for apoptosis analysis by an Annexin V-PI detection kit. As can be seen from the results (Figs. 5a and 5b), there is only a small increase in the percentage of cells treated with CDDP alone undergoing apoptosis compared to the control (3.96% vs. 3.17%). When cells were treated with Ethaselen and CDDP, a significant increase was observed in the percentage of Annexin V+/PI- cells (Fig. 5c), indicating an early stage apoptosis induced by the addition of a small amount of Ethaselen.

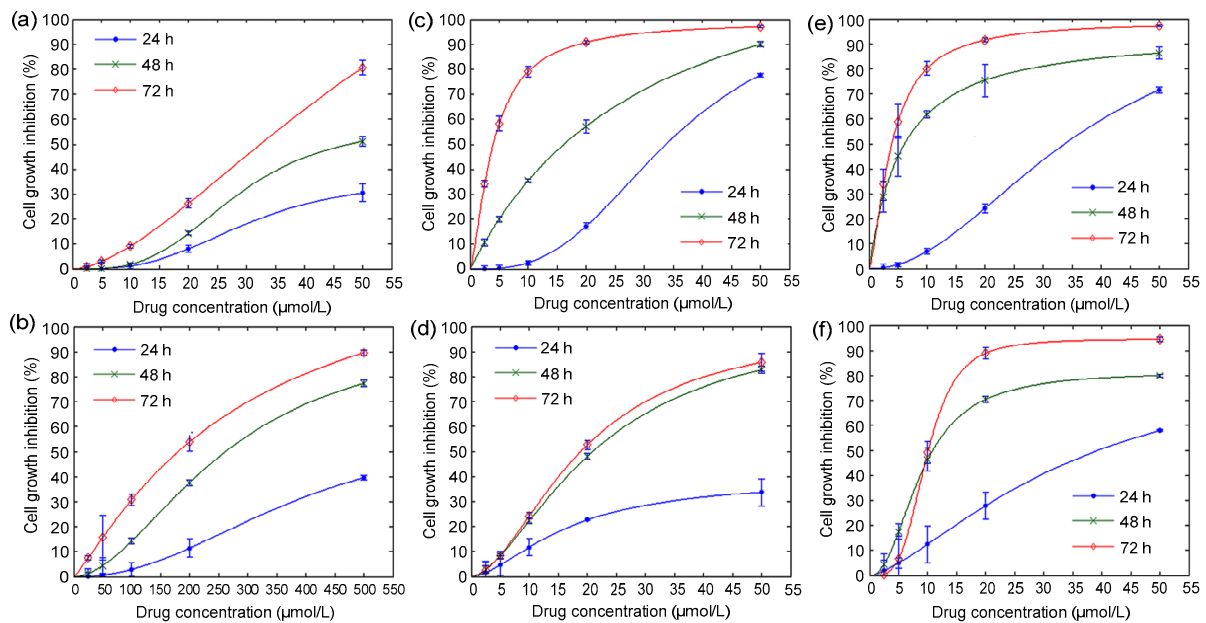


Fig. 4 Cell growth inhibition curves of K562 and K562/CDDP cells treated with CDDP, Ethaselen, or their combination (the concentration of Ethaselen in combination was fixed at 1/10 of CDDP concentration)

(a) Dose-response curves of K562 after treatment with CDDP for 24, 48, and 72 h. (b) Dose-response curves of K562/CDDP after treatment with CDDP for 24, 48, and 72 h. (c) Dose-response curves of K562 after treatment with Ethaselen for 24, 48, and 72 h. (d) Dose-response curves of K562/CDDP after treatment with Ethaselen for 24, 48, and 72 h. (e) Dose-response curves of K562 after treatment with CDDP+Ethaselen for 24, 48, and 72 h. (f) Dose-response curves of K562/CDDP after treatment with CDDP+Ethaselen for 24, 48, and 72 h

Table 2 Inhibitory effects of CDDP, Ethaselen, and their combination on K562 and K562/CDDP after treatment for 48 h

Cell line	Inhibitory effect IC ₅₀ (%) [*]			CI
	CDDP	Ethaselen	CDDP+Ethaselen (10:1)	
K562	48.748±0.697	15.270±3.313	6.255±0.664	0.169 (synergism)
K562/CDDP	260.986±6.898	20.694±1.814	12.368±1.611	0.107 (synergism)
<i>P</i> -value	<0.01	<0.01	<0.01	

IC₅₀: half-maximum inhibitory concentration; CI: combination index. ^{*} Data are expressed as mean±SD (n=3)

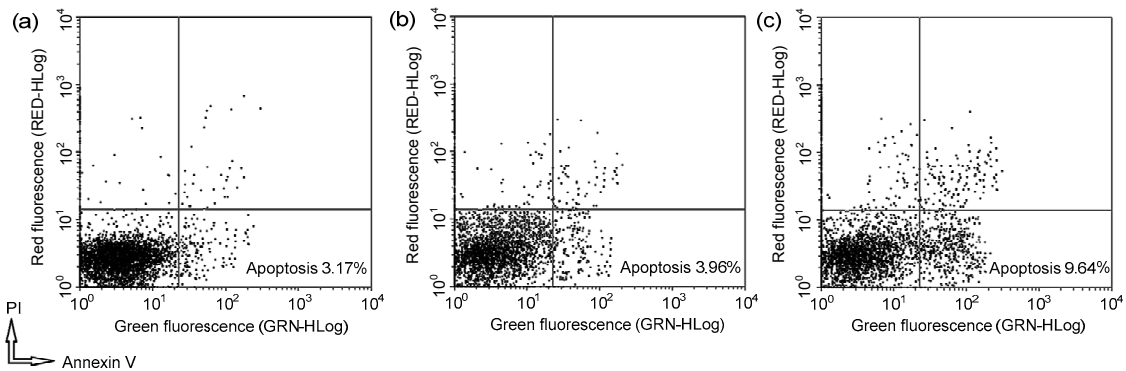


Fig. 5 Flow cytometric analysis of apoptosis of K562/CDDP cells

(a) Apoptosis analysis of K562/CDDP cells treated with vehicle (control) for 24 h. (b) Apoptosis analysis of K562/CDDP cells treated with 50 $\mu\text{mol/L}$ CDDP for 24 h. (c) Apoptosis analysis of K562/CDDP cells treated with the combination of 1.5 $\mu\text{mol/L}$ Ethaselen and 15 $\mu\text{mol/L}$ CDDP for 24 h

3.5 Intracellular ROS content detection

As shown in Fig. 6, the ROS level in K562/CDDP cells was twice of that in K562 cells. Exposure to CDDP resulted in an increase of the ROS levels in K562, while this increase was not obvious in K562/CDDP. By using the combination of CDDP and small amounts of Ethaselen, the ROS level further increased in both K562 and K562/CDDP cells, which was significantly different ($P < 0.05$) from that with CDDP treatment alone. These results (Fig. 6) indicate that the degree of tolerance for ROS in K562/CDDP cells and the failure of inducing ROS by CDDP may partly be the cause of cisplatin resistance. In addition, further inducing the increase of ROS will reverse the cisplatin resistance in K562/CDDP cells.

3.6 Western blot analysis for the expressions of Bax, Bcl-2, Caspase-3, and cytochrome *c* in K562 and K562/CDDP cells after different treatments

Release of cytochrome *c* is associated with the decrease of Bcl-2 and increase of Bax followed by activating Caspase-9 and Caspase-3 (Rossé *et al.*, 1998; Jia *et al.*, 2015). Compared to K562 cells, as shown in Figs. 7 and 8, a tiny increase in the expression of Bcl-2 and a small decrease in the expression of Bax in K562/CDDP cells were observed. Western blot analysis revealed that Bax protein level of K562 was significantly increased by CDDP alone compared to K562/CDDP cells, while Bcl-2 protein expression in K562 treated by CDDP alone was significantly suppressed compared to that in K562/CDDP cells (Figs. 7 and 8). Hence, the increased ratio of Bax to Bcl-2 protein after CDDP treatment, following the

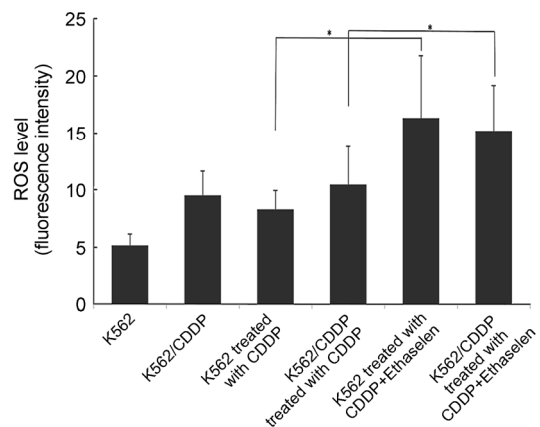


Fig. 6 Level of intracellular ROS in K562 and K562/CDDP cells pre-incubated with vehicle (control), 50 $\mu\text{mol/L}$ CDDP, or the combination of 1.5 $\mu\text{mol/L}$ Ethaselen and 15 $\mu\text{mol/L}$ CDDP for 24 h ($P < 0.05$)

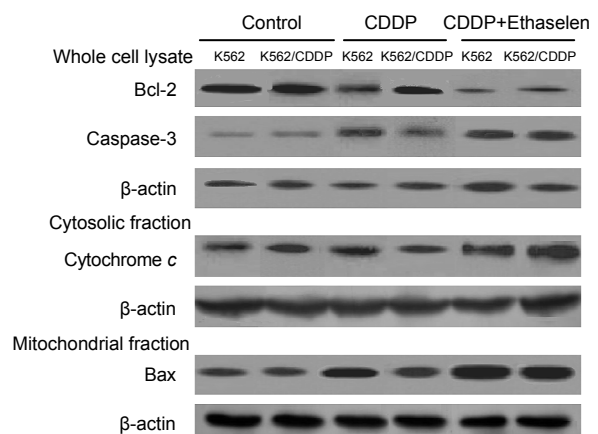


Fig. 7 Western blot analysis for the effects of different drug groups on the expressions of Bax, Bcl-2, Caspase-3, and cytochrome *c* in K562 and K562/CDDP cells pre-incubated with vehicle (control), 50 $\mu\text{mol/L}$ CDDP or the combination of 1.5 $\mu\text{mol/L}$ Ethaselen and 15 $\mu\text{mol/L}$ CDDP for 24 h

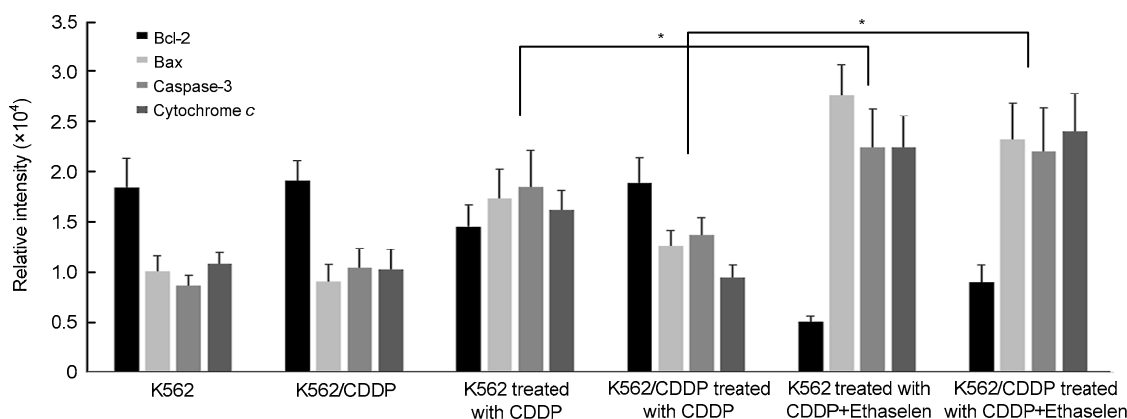


Fig. 8 Relative intensity of the expressions of Bax, Bcl-2, Caspase-3, and cytochrome *c* in K562 and K562/CDDP cells. Data are expressed as mean±SD ($n=3$). * $P<0.05$

cytochrome *c* release and Caspase pathway activation in K562 cells, was not seen in K562/CDDP cells. This result suggests that the ratio of pro-apoptotic drive to anti-apoptotic drive, as revealed by the ratio of Bax to Bcl-2 protein, may determine the difference in CDDP-induced apoptosis between K562 and K562/CDDP cells. By the combined CDDP-Ethaselen treatment, the ratio of Bax/Bcl-2 was obviously increased, subsequently inducing cytochrome *c* release from mitochondria to cytosol and Caspase-3 activation in both K562 and K562/CDDP cells. These results indicated that Ethaselen could reverse cisplatin resistance in drug-resistant K562 cells via activating the mitochondria-mediated intrinsic pathway.

3.7 Enhanced mitochondrial membrane permeability by the formation of permeability transition pores, following the cytochrome *c* release

As mitochondrial membrane permeability (MMP) is enhanced by the formation of permeability transition pores (PTPs), which are triggered by ROS, and CsA (a PTP inhibitor) was used to block the formation of PTPs in this study. As shown in Figs. 9 and 10, whether or not adding CsA, there was no obvious difference in cytochrome *c* release in K562/CDDP after exposure to CDDP alone, which confirmed that CDDP cannot induce the increase in the ROS level (Fig. 6), followed by the failure of PTP formation in K562/CDDP cells. The treatment of CDDP and Ethaselen triggered the release of cytochrome *c*, which was blocked by the treatment with CsA, suggesting that the cytochrome *c* release depends, at least partially, on the formation of PTPs. This result further

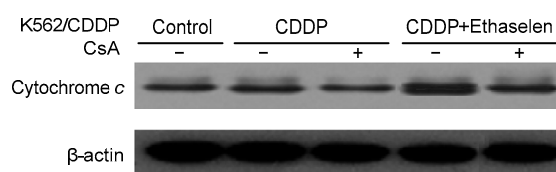


Fig. 9 Western blot analysis for the effects with or without adding 15 $\mu\text{mol/L}$ CsA on the expression of cytochrome *c* in K562/CDDP cells after the treatment of vehicle (control), 50 $\mu\text{mol/L}$ CDDP, or the combination of 1.5 $\mu\text{mol/L}$ Ethaselen and 15 $\mu\text{mol/L}$ CDDP for 24 h

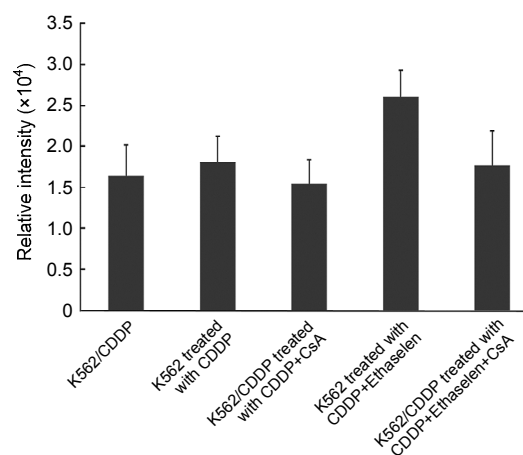


Fig. 10 Relative intensity of the expression of cytochrome *c* in K562/CDDP cells

Data are expressed as mean±SD ($n=3$)

confirmed that Ethaselen reversing cisplatin resistance by inducing apoptosis is initiated by the release of cytochrome *c* from mitochondria, suggesting that the increase in ROS level may directly trigger the formation of PTPs to disrupt mitochondrial membrane integrity in a Bcl-2-independent manner.

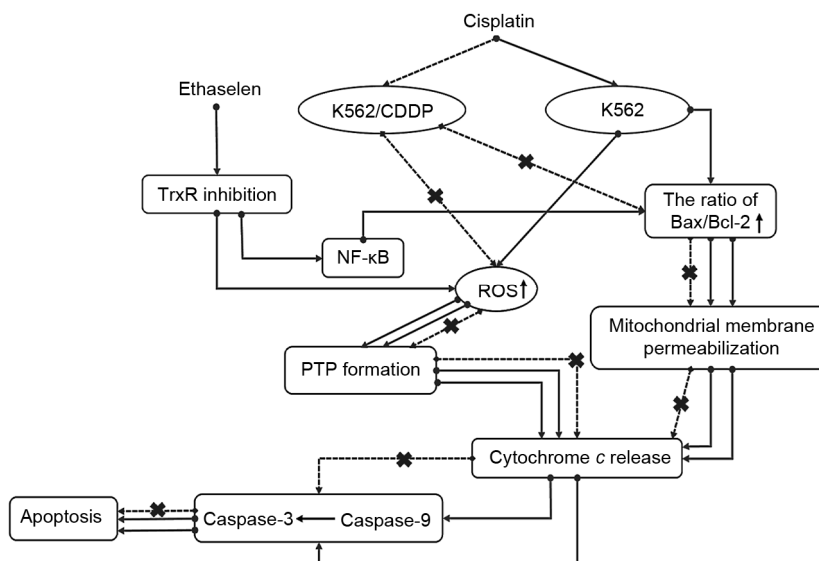


Fig. 11 Potential mechanisms of reversal of cisplatin resistance by Etheselen in cisplatin-resistant K562 cells

4 Conclusions

A potent and efficient way to reverse cisplatin resistance in K562/CDDP cells by Etheselen was observed and confirmed through the 21 times decline of the IC_{50} of CDDP in K562/CDDP cells by adding small amounts of Etheselen. The investigation of apoptosis-related molecules and mitochondrial-function-related factors further indicated two possible ways to reverse cisplatin resistance (Fig. 11):

1. Etheselen can specifically inhibit TrxR activities, resulting in the reduction of nuclear factor κB (NF- κB) activities (Lan *et al.*, 2007), followed by the upregulation of Bax and downregulation of Bcl-2. The increased ratio of Bax/Bcl-2 subsequently induces cytochrome *c* release from mitochondria to cytosol and Caspase-3 activation in K562/CDDP cells.

2. The elevated ROS levels in K562/CDDP through the inhibition of TrxR by Etheselen can trigger the formation of PTPs and then enhance MMP, which further confirms that Etheselen reversing cisplatin resistance by inducing apoptosis is initiated by the release of cytochrome *c* from mitochondria in a Bcl-2-independent manner.

Our results shed new light on a comprehensive understanding of the mechanism of CDDP resistance in K562 cells and a better knowledge of the relationship between CDDP resistance and Etheselen-

induced changes of TrxR, ROS, and apoptosis-related molecules, providing an efficient way to reverse cisplatin resistance in drug-resistant K562 cells by Etheselen. Future studies should be carried out such as observing the reversing effects on some other cells to further confirm our conclusion and exploring the best ratio of Etheselen and cisplatin in combination treatment to provide a potential clinical application of Etheselen-cisplatin combined chemotherapy.

Compliance with ethics guidelines

Suo-fu YE, Yong YANG, Lin WU, Wei-wei MA, and Hui-hui ZENG declare that they have no conflict of interest.

This article does not contain any studies with human or animal subjects performed by any of the authors.

References

- Bargou, R.C., Bommert, K., Weinmann, P., *et al.*, 1995. Induction of Bax- α precedes apoptosis in a human B lymphoma cell line: potential role of the *bcl-2* gene family in surface IgM-mediated apoptosis. *Eur. J. Immunol.*, **25**(3):770-775. <http://dx.doi.org/10.1002/eji.1830250322>
- Chao, C.C., Huang, S.L., Huang, H.M., *et al.*, 1991. Cross-resistance to UV radiation of a cisplatin-resistant human cell line: overexpression of cellular factors that recognize UV-modified DNA. *Mol. Cell. Biol.*, **11**(4):2075-2080. <http://dx.doi.org/10.1128/MCB.11.4.2075>
- Chen, J., Li, H.M., Zhang, X.N., *et al.*, 2014. Dioscin-induced apoptosis of human LNCaP prostate carcinoma cells through activation of caspase-3 and modulation of Bcl-2

- protein family. *J. Huazhong Univ. Sci. Technol. Med. Sci.*, **34**(1):125-130.
<http://dx.doi.org/10.1007/s11596-014-1243-y>
- Chu, G., 1994. Cellular responses to cisplatin. The roles of DNA-binding proteins and DNA repair. *J. Biol. Chem.*, **269**(2):787-790.
- Du, J.P., Chen, P., Fei, H.X., et al., 2007. Establishment of adriamycin-resistant and cisplatin-resistant gastric cancer cell lines and assessment on their sustainability of drug resistance. *Chin. J. Gastroenterol. Hepatol.*, **16**(4):368-372 (in Chinese).
<http://dx.doi.org/10.3969/j.issn.1006-5709.2007.04.022>
- Dumay, A., Laulier, C., Bertrand, P., et al., 2006. Bax and Bid, two proapoptotic Bcl-2 family members, inhibit homologous recombination, independently of apoptosis regulation. *Oncogene*, **25**(22):3196-3205.
<http://dx.doi.org/10.1038/sj.onc.1209344>
- Fu, J.N., Li, J., Tan, Q., et al., 2011. Thioredoxin reductase inhibitor etahaselen increases the drug sensitivity of the colon cancer cell line LoVo towards cisplatin via regulation of G1 phase and reversal of G2/M phase arrest. *Invest. New Drugs*, **29**(4):627-636.
<http://dx.doi.org/10.1007/s10637-010-9401-y>
- Hahn, P., Lindsten, T., Ying, G.S., et al., 2003. Proapoptotic Bcl-2 family members, Bax and Bak, are essential for developmental photoreceptor apoptosis. *Invest. Ophthalmol. Vis. Sci.*, **44**(8):3598-3605.
<http://dx.doi.org/10.1167/iov.02-1113>
- Harrington, C.F., le Pla, R.C., Jones, G.D., et al., 2010. Determination of cisplatin 1,2-intrastrand guanine-guanine DNA adducts in human leukocytes by high-performance liquid chromatography coupled to inductively coupled plasma mass spectrometry. *Chem. Res. Toxicol.*, **23**(8):1313-1321.
<http://dx.doi.org/10.1021/tx100023c>
- Haslehurst, A.M., Koti, M., Dharsee, M., et al., 2012. EMT transcription factors snail and slug directly contribute to cisplatin resistance in ovarian cancer. *BMC Cancer*, **12**:91.
<http://dx.doi.org/10.1186/1471-2407-12-91>
- Heath-Engel, H.M., Chang, N.C., Shore, G.C., 2008. The endoplasmic reticulum in apoptosis and autophagy: role of the BCL-2 protein family. *Oncogene*, **27**(50):6419-6433.
<http://dx.doi.org/10.1038/onc.2008.309>
- Jia, G., Wang, Q., Wang, R., et al., 2015. Tubeimoside-1 induces glioma apoptosis through regulation of Bax/Bcl-2 and the ROS/Cytochrome C/Caspase-3 pathway. *Oncotargets Ther.*, **8**:303-311.
<http://dx.doi.org/10.2147/OTT.S76063>
- Lan, L., Zhao, F., Wang, Y., et al., 2007. The mechanism of apoptosis induced by a novel thioredoxin reductase inhibitor in A549 cells: possible involvement of nuclear factor- κ B-dependent pathway. *Eur. J. Pharmacol.*, **555**(2-3):83-92.
<http://dx.doi.org/10.1016/j.ejphar.2006.10.037>
- Mantri, Y., Lippard, S.J., Baik, M.H., 2007. Bifunctional binding of cisplatin to DNA: why does cisplatin form 1,2-intrastrand cross-links with AG but not with GA? *J. Am. Chem. Soc.*, **129**(16):5023-5030.
<http://dx.doi.org/10.1021/ja067631z>
- Miyata, Y., Nomata, K., Ohba, K., et al., 2012. Use of low-dose combined therapy with gemcitabine and paclitaxel for advanced urothelial cancer patients with resistance to cisplatin-containing therapy: a retrospective analysis. *Cancer Chemother. Pharmacol.*, **70**(3):451-459.
<http://dx.doi.org/10.1007/s00280-012-1938-3>
- Oiso, S., Takayama, Y., Nakazaki, R., et al., 2014. Factors involved in the cisplatin resistance of KCP-4 human epidermoid carcinoma cells. *Oncol. Rep.*, **31**(2):719-726.
<http://dx.doi.org/10.3892/or.2013.2896>
- Rossé, T., Olivier, R., Monney, L., et al., 1998. Bcl-2 prolongs cell survival after Bax-induced release of cytochrome c. *Nature*, **391**(6666):496-499.
<http://dx.doi.org/10.1038/35160>
- Sainz, R.M., Mayo, J.C., Tan, D.X., et al., 2003. Antioxidant activity of melatonin in Chinese hamster ovarian cells: changes in cellular proliferation and differentiation. *Biochem. Biophys. Res. Commun.*, **302**(3):625-634.
[http://dx.doi.org/10.1016/S0006-291X\(03\)00230-4](http://dx.doi.org/10.1016/S0006-291X(03)00230-4)
- Shi, C., Yu, L., Yang, F., et al., 2003. A novel organoselenium compound induces cell cycle arrest and apoptosis in prostate cancer cell lines. *Biochem. Biophys. Res. Commun.*, **309**(3):578-583.
<http://dx.doi.org/10.1016/j.bbrc.2003.08.032>
- Tan, Q., Li, J., Yin, H.W., et al., 2010. Augmented antitumor effects of combination therapy of cisplatin with etahaselen as a novel thioredoxin reductase inhibitor on human A549 cell in vivo. *Invest. New Drugs*, **28**(3):205-215.
<http://dx.doi.org/10.1007/s10637-009-9235-7>
- Tanaka, S., Wakeyama, H., Akiyama, T., et al., 2010. Regulation of osteoclast apoptosis by Bcl-2 family protein Bim and Caspase-3. *Adv. Exp. Med. Biol.*, **658**:111-116.
http://dx.doi.org/10.1007/978-1-4419-1050-9_12
- Tao, X.J., Tilly, K.I., Maravei, D.V., et al., 1997. Differential expression of members of the bcl-2 gene family in proliferative and secretory human endometrium: glandular epithelial cell apoptosis is associated with increased expression of bax. *J. Clin. Endocrinol. Metab.*, **82**(8):2738-2746.
<http://dx.doi.org/10.1210/jcem.82.8.4146>
- Tilly, J.L., Tilly, K.I., Kenton, M.L., et al., 1995. Expression of members of the bcl-2 gene family in the immature rat ovary: equine chorionic gonadotropin-mediated inhibition of granulosa cell apoptosis is associated with decreased bax and constitutive bcl-2 and bcl-xlong messenger ribonucleic acid levels. *Endocrinology*, **136**(1):232-241.
<http://dx.doi.org/10.1210/endo.136.1.7828536>
- Torigoe, T., Izumi, H., Ishiguchi, H., et al., 2005. Cisplatin resistance and transcription factors. *Curr. Med. Chem. Anticancer Agents*, **5**(1):15-27.

- <http://dx.doi.org/10.2174/1568011053352587>
Wang, L., Fu, J.N., Wang, J.Y., et al., 2011. Selenium-containing thioredoxin reductase inhibitor ethaselen sensitizes non-small cell lung cancer to radiotherapy. *Anticancer Drugs*, **22**(8):732-740.
<http://dx.doi.org/10.1097/CAD.0b013e32834618bc>
Wang, L., Yang, Z., Fu, J., et al., 2012. Ethaselen: a potent mammalian thioredoxin reductase 1 inhibitor and novel organoselenium anticancer agent. *Free Radic. Biol. Med.*, **52**(5):898-908.
<http://dx.doi.org/10.1016/j.freeradbiomed.2011.11.034>
Xing, F., Li, S., Ge, X., et al., 2008. The inhibitory effect of a novel organoselenium compound BBSKE on the tongue cancer Tca8113 in vitro and in vivo. *Oral Oncol.*, **44**(10):963-969.
<http://dx.doi.org/10.1016/j.oraloncology.2007.12.001>
Yaneva, J.N., Paneva, E.G., Zacharieva, S.L., et al., 2007. Histone H1 interacts preferentially with DNA fragments containing a cisplatin-induced 1,2-intrastrand cross-link. *Z. Naturforsch. C*, **62**(11-12):905-908.
<http://dx.doi.org/10.1515/znc-2007-11-1220>
Yeh, K.H., Cheng, A.L., 1997. High-dose tamoxifen reverses drug resistance to cisplatin and etoposide in a patient with advanced large cell carcinoma of lung. *Anticancer Res.*, **17**(2B):1341-1343.
Zhao, F., Yan, J., Deng, S., et al., 2006. A thioredoxin reductase inhibitor induces growth inhibition and apoptosis in five cultured human carcinoma cell lines. *Cancer Lett.*, **236**(1):46-53.
<http://dx.doi.org/10.1016/j.canlet.2005.05.010>
Zheng, S., Zhao, M., Ren, Y., et al., 2015. Sesamin suppresses STZ induced INS-1 cell apoptosis through inhibition of NF- κ B activation and regulation of Bcl-2 family protein expression. *Eur. J. Pharmacol.*, **750**:52-58.
<http://dx.doi.org/10.1016/j.ejphar.2015.01.031>

中文概要

题目: 硫氧还蛋白还原酶抑制剂乙烷硒啉逆转顺铂耐药及其机制研究

目的: 研究凋亡调控相关蛋白来了解顺铂耐药成因,同时考察乙烷硒啉(Ethaselen)在 K562 耐药细胞中逆转顺铂耐药的作用,并初步探讨其作用机制。

创新点: 首次研究乙烷硒啉在逆转顺铂耐药中的作用,且此作用与乙烷硒啉诱导细胞凋亡相关。

方法: 通过长时间脉冲诱导得到顺铂耐药 K562 细胞,并观察耐药细胞形态及倍增时间。采用 MTT 法考察乙烷硒啉、顺铂及其联用组在不同细胞株间的生长抑制作用。流式细胞术分析细胞凋亡情况以及细胞内活性氧(ROS)水平。最后,通过蛋白质免疫印迹(Western blot)考察凋亡调控相关蛋白水平的变化。

结论: 脉冲诱导得到的 K562 耐药细胞对顺铂的耐受性是原 K562 细胞的 5.34 倍。形态学观察发现,耐药细胞体积增大,粘附性进一步降低。乙烷硒啉与顺铂联用表现出协同效应。当加入少量的乙烷硒啉(顺铂与乙烷硒啉的摩尔比率为 10:1),顺铂作用 K562 耐药细胞的半抑制浓度(IC₅₀)值可以减少 21 倍。流式细胞术及 Western blot 表明,乙烷硒啉能够诱导耐药细胞凋亡。其逆转顺铂耐药主要是通过调控 Bcl-2 及 Bax 蛋白比例以及通过提高细胞内活性氧水平引起线粒体通透转运孔道(PTP)蛋白孔道的形成来促使释放细胞色素 c,进而引起 Caspase 凋亡途径。

关键词: 乙烷硒啉; 顺铂耐药; K562; 凋亡; Bcl-2